The 8190-¿ sodium doublet in cataclysmic variables - IV. A survey of 22 objects

Article (Published Version)

Mon. Not. R. Astron. Soc. **287,** 271–286 (1997)

The 8190-Å sodium doublet in cataclysmic variables – IV. A survey of 22 objects

Robert Connon Smith,[1] M. J. Sarna,[1★] M. S. Catalán[2] and D. H. P. Jones[3]

[1]*Astronomy Centre, School of Mathematical and Physical Sciences, University of Sussex, Falmer, Brighton BN1 9QH*
[2]*Department of Physics and Astronomy, University of St Andrews, North Haugh, St Andrews, Fife KY16 9SS*
[3]*Royal Greenwich Observatory, Madingley Road, Cambridge CB3 0EZ*

Accepted 1996 December 14. Received 1996 November 14; in original form 1996 July 12

ABSTRACT

A survey of 22 known and suspected cataclysmic variables has been carried out with the 4.2-m WHT on La Palma, using ISIS to provide coverage of most of the optical spectrum. 10 faint stars (UU Aql, AT Cnc, EY Cyg, CG Dra, LL Lyr, NN Ser, BC UMa, DV UMa, TW Vir and RE J1629+780) and one bright one (Z Cam) show red dwarf features in the spectrum. For UU Aql, EY Cyg, LL Lyr and TW Vir, this is the first direct spectroscopic detection of the red dwarf. For all these systems we have determined the most probable spectral type of the secondary star. In addition we find marginal evidence of the red dwarf in V391 Lyr, SW UMa and PQ Gem (=RE J0751+144). Allowing for selection effects, the proportion of systems that show evidence of the red dwarf is larger than that found in an earlier survey of brighter objects.

Key words: surveys – stars: individual: EY Cyg – stars: individual: UU Aql – stars: individual: LL Lyr – stars: individual: TW Vir – novae, cataclysmic variables.

1 INTRODUCTION

In 1988 Friend et al. (1988) published the results of the first large-scale survey of cataclysmic variables (CVs) that covered the red part of the spectrum. This survey revealed direct spectroscopic evidence of the red dwarf in about one quarter (16) of the 65 systems surveyed. In the northern hemisphere, the survey was carried out using the 2.5-m Isaac Newton Telescope and was therefore restricted to relatively bright systems. When the ISIS spectrograph became available on the 4.2-m William Herschel Telescope (WHT), we proposed a further survey, of fainter objects, to improve the statistics and to find new systems for detailed study. The new survey, which we present here, covers a much larger range of wavelength than the previous one, at a somewhat lower resolution.

In most cases, only a few spectra were taken of each target. However for NN Ser, a suspected pre-cataclysmic variable, orbital coverage was obtained. The NN Ser data have been published separately (Catalán et al. 1994), as have the spectra of BH Lyn, which were combined with a more extensive set of blue spectra to confirm that the earlier spectra had been taken during an unusual low state (Dhillon et al. 1992). In addition, the binary RE J1629+780 has been found to be a detached white dwarf–red dwarf system (Cooke et al. 1992) and therefore has been the subject of a separate analysis by Catalán et al. (1995). The other spectra will be presented here. Some preliminary results were shown at the Abano CV meeting (Smith, Sarna & Jones 1995).

★Present address: Nicolaus Copernicus Astronomical Center, ul. Bartycka 18, 00–716 Warsaw, Poland.

Two of our targets, EI UMa (PG 0834+488) and V589 Her, look completely different from a typical cataclysmic variable spectrum. They show no emission lines and their spectra are dominated solely by absorption features suggesting, in both cases, a single red star possibly of spectral type G or K. Since we suspect that we may have misidentified both stars at the telescope, we have chosen not to include these stars in our analysis.

2 OBSERVATIONS AND DATA REDUCTION

2.1 Observations

We obtained 150 spectra of 22 cataclysmic or suspected cataclysmic variables on the nights of 1991 April 27 to May 1, using the ISIS triple-beam spectrograph at the Cassegrain focus of the 4.2-m WHT at the Roque de los Muchachos Observatory on the island of La Palma. The journal of observations is given in Table 1, where Night of Observation 1 = 1991 April 27/28 and so on. The seeing was poor (several arcsec) on nights 1 to 3.

The low-dispersion 158 line mm^{-1} gratings were used on both arms. With EEV CCDs and the 5670 dichroic, this gave a wavelength coverage in the range 3450–5550 Å in the blue and 5810–8910 Å in the red, at a resolution of 5–6 Å. The slit width was 0.9 arcsec, and the slit was maintained at the parallactic angle throughout each exposure.

A copper–argon/copper–neon arc spectrum was taken at every new star position, and at 1- or 2-h intervals during the observation of those stars for which many spectra were taken, to provide wavelength calibration and to correct for instrumental flexure and

Table 1. Journal of spectroscopic observations, in lexigraphical order.

Name of object	Night of Observation	Number of Spectra	Exposure Time (s)	Type	Orbital Period (hr)	Remarks
UU Aql	1	1B 1R	500	UG	3.37?	Red star detected
	2	2B 2R	500/1000			
Z Cam	1	2B 2R	300/600	ZC	6.96	Red star detected
YZ Cnc	4	4B 4R	300	SU	2.08	
AT Cnc	2	2B 2R	500	ZC	5.73	Red star detected
	3	3B 3R	500			
EY Cyg	1	1B 1R	1000	UG	5.24	Red star detected
V503 Cyg	2	1B 1R	1024	SU	1.83	
CG Dra	4	1B 1R	1000	UG	–	Red star detected
PQ Gem	2	3B 3R	500	IP/AM?	5.3?	
(RE J0751+144)	3	3B 3R	500			
V589 Her	2	2B 2R	1000	UG	–	Red star only?
BH Lyn[1]	4	5B 5R	500	NL	3.74	
LL Lyr	4	3B 3R	1024	UG	–	Red star detected
V 391 Lyr	4	3B 3R	1024	ZC	–	
NN Ser[2]	1	6B 6R	1000/2000	DS	3.12	Red star detected
	3	10B 10R	1000			
SU UMa	4	4B 4R	100/300	SU	1.83	
SW UMa	4	1B 1R	300	SU	1.36	
AN UMa	2	3B 3R	1024	AM	1.91	
BC UMa	3	2B 2R	1000	SU	1.51	Red star detected
DV UMa	4	2B 2R	1000	UG/SU	2.06	Red star detected
EI UMa (PG 0834+488)	1	2B 1R	1000	NL/UG/DQ?	6.43	Red star only?
SS UMi	1	2B 2R	1000/1024	SU	1.63	
TW Vir	1	1B 1R	1000	UG	4.38	Red star detected
	4	2B 2R	500			
RE J1629+780[3]	2	3B 2R	1024	DS	> 2.5	Red star detected
	4	2B 2R	500/512			

B – blue band: wavelength range λλ3450–5550 Å.
R – red band: wavelength range λλ5810–8910 Å.
Type taken from GCVS (Kholopov 1985) or Ritter & Kolb (1993) unless otherwise cited in the text.
Period from Ritter & Kolb (1993) unless otherwise cited in the text or in the papers cited in the table.
[1]Dhillon et al. (1992).
[2]Catalán et al. (1994).
[3]Catalán et al. (1995).

stability. Spectra of the spectrophotometric standards HD 84937 and BD+26°2606 (Oke & Gunn 1983) were also taken in order to remove the telluric absorption features and correct for instrumental wavelength response. 10 single red dwarfs in the spectral-type range K5 to M8 were observed to allow spectral-type calibration.

2.2 Data reduction

The data reduction can be divided into two- and one-dimensional stages. After bias subtraction and division by the flat-field to correct for medium-scale sensitivity variations of the detector, optimal extraction (Horne 1986) as implemented by the FIGARO software package was used to reduce the two-dimensional images to one-dimensional spectra. The arc spectra were extracted from the same region on the detector as the objects and used to obtain wavelength calibration to an accuracy of about 0.1 Å. Telluric absorption lines were removed by division by a wavelength-calibrated template produced from the observed flux standard stars. This step is essential if there is to be any hope of detecting the Na I doublet near 8200 Å, or the red TiO bands, all of which lie close to strong telluric features (see, for example, table 5 of Kirkpatrick, Henry & McCarthy 1991 and figs 2 to 6 of Zwitter & Munari 1994). Having removed atmospheric features, the spectra were corrected for the variations of instrumental response with wavelength and for large-scale sensitivity variations by multiplying by a calibration spectrum produced from the FIGARO tables of the Oke & Gunn standards. There were no comparison stars on the same slit for any of our objects, so absolute fluxes are not available. We have not attempted to correct for interstellar reddening.

3 SYSTEMS THAT SHOW RED DWARF FEATURES

We have obtained spectra of 21 faint CVs and one bright one at low resolution. Of the faint systems, 10 show red dwarf features with a good degree of certainty, and three exhibit marginal signs of the presence of the cool component. We discuss eight of these systems first, omitting the detached systems NN Ser and RE J1629+780, whose spectra have been published elsewhere (Catalán et al. 1994, 1995). We also present the spectrum of the bright system, Z Cam. For consistency, we identify the TiO bands by the wavelengths of their blue bandheads, as given by Kirkpatrick et al. (1991), even if the position of the bandhead is not readily seen on the spectrum. We summarize the list of identified lines, their equivalent widths and total fluxes in the Appendix.

Table 2. Ratio of the integrated flux for the TiO bands at λλ7165 and 7665 Å and the TiO band at λ7665 Å relative to the continuum flux at λ7500 Å together with the spectral type that corresponds to those values. See text for comments.

Object	TiO ratio $\frac{d_\nu(\lambda7665)}{d_\nu(\lambda7165)}$	TiO/Continuum $\frac{d_\nu(\lambda7665)}{c_\nu(\lambda7500)}$	Corresponding spectral type
UU Aql	0.58 ± 0.07	0.04 ± 0.01	M2–4V
LL Lyr	0.66 ± 0.05	0.13 ± 0.07	M3–4V
BC UMa	2.46 ± 0.80	0.16 ± 0.05	M5 or later
DV UMa	1.05 ± 0.17	0.21 ± 0.05	M4–5V
TW Vir	2.24 ± 0.30	0.04 ± 0.01	M5–6V

For the majority of the objects it was possible to obtain an initial estimate of the spectral type of the secondary star using the TiO band flux ratios as employed by Wade & Horne (1988). Since our far-red data have practically the same spectral resolution as theirs, although covering a slightly larger wavelength range, we used the same integration limits. This allowed us to compare our results with their M dwarf standard star measurements (see fig. 4 in Wade & Horne 1988). Our derived TiO ratios are summarized in Table 2. However, it is important to note that this technique is not sensitive to late-K or early-M dwarfs where the TiO bands are barely visible. Therefore, to classify the cool components in Z Cam, AT Cnc, EY Cyg and CG Dra other techniques were used. These are discussed separately for each object.

3.1 UU Aql

UU Aql is a U Gem-type dwarf nova, with a *V* magnitude in quiescence in the range 16.1 to 16.7. The time between outbursts (about 71 d) shows a regular variability, interpreted by Bianchini (1990) as evidence for a 'solar cycle' with a period of 12.9 yr; however, Andronov & Shakun (1990) argue that the data are better fitted by an alternation between two inter-outburst periods. Richman, Applegate & Patterson (1994) discuss the data for many stars, and prefer a solar-cycle interpretation, although rejecting any strict periodicity.

There have been few time-resolved observations of UU Aql on a shorter time-scale and its orbital period is uncertain. It was observed in quiescence by Szkody (1987) in *UBV* photometry who gave the orbital period as 202 or 236 min. Based on a private communication from Thorstensen, the catalogues of Ritter (1990) and Ritter & Kolb (1993) quote 202.3 min, while Shafter (1992) gives 236 min as the preferred value. Bianchini (1990), on the other hand, quotes a shorter orbital period of 1.88 h (113 min).

Our spectra (Fig. 1) were taken at the end of an outburst, as can be seen by the weakening of the Balmer absorption lines between nights 1 (upper panel) and 2 (lower panel). The flux level in the continuum is also lower on night 2, although the absolute flux is not reliable. On the second night the Na I doublet near 8200 Å and the TiO bands redward of 7053 and 7666 Å were detected. This is the first published spectral evidence for the red dwarf component, although Antipova (1987) claimed evidence for a secondary without giving a reference. In addition to the lines quoted in the Appendix, we have detected an emission feature at 5167 Å which corresponds to Mg I. Our analysis of the TiO band ratios gives a spectral type in the range M2–4 using a single spectrum from night 2. We picked the one with the longest exposure time and thus the highest signal-to-noise (S/N) ratio, which also happens to be the one furthest in time from the outburst. Nevertheless, this estimate is quite preliminary since the contribution of the secondary star to the continuum was found to be only about 20 per cent (Table 2 – see fig. 4 of Wade & Horne 1988 for the calibration), and although the formal errors are small it is likely that the effects of the outburst on the red star are not negligible. Furthermore, there is a prominent dip near the TiO band near 7165 Å which may be an artefact of the data reduction stage.

3.2 TW Vir

This U Gem system was placed on our target list because the secondary had been detected via ellipsoidal variations in the infrared (at *H*) by Mateo, Szkody & Bolte (1985). They deduced a spectral type of M2–4V by assuming the star to fill its Roche lobe and to obey a main-sequence mass–radius relation.

Our spectra (Fig. 1) show a large change in appearance between nights 1 (top panel) and 4 (bottom panel), with the emission component of the Balmer lines all but disappearing. In the night 1 spectrum, there is already the beginning of a broad absorption component apparent, especially in Hγ, and these components become dominant by night 4. We have clearly caught the system on the rise to outburst, although the rise seems to have taken several days, which is much slower than observed by Mansperger & Kaitchuck (1990) two years earlier.

The data show signs of the secondary star. We detect weak absorption lines in the position of the Na I doublet near 8190 Å on both nights. Using the single spectrum taken on night 1, which was on the rise to outburst, we derive a spectral type for the secondary of between M5 and M6, much later than suggested by Mateo et al. (1985). Given that the orbital period has been determined to be 4.33 h, if our estimate is correct, this implies a fairly expanded secondary star. However, since we have obviously caught the object while it was brightening, it is probable that our result is somewhat biased by the presence of a bright disc.

Higher Balmer series emission lines are present in the spectrum (Fig. 1) all the way up to H9, with the Ca II H line appearing blended with Hϵ in night 1. Similarly, in the far-red, the Ca II emission lines at λλ8498 and 8545 Å are blended with Paschen 12 and 11, respectively. There is a possible P Cygni profile in Hα, suggesting a wind, which may be stronger during outburst.

As with UU Aql, Mg I at λ5167 Å is evident in the night 1 spectrum, as is the O I emission triplet at λ7773 Å. However, the Mg I line is absent in the spectra taken on night 4, while the O I line actually goes into absorption. Therefore, on night 4, both O I and Na I were detected in absorption. This is quite an unusual configuration of lines, previously seen only in the outburst spectrum of IP Peg (Martin et al. 1989) and in Z Cha (Wade & Horne 1988). Friend et al. (1988) found in their far-red spectroscopic survey of CVs that secondary absorption features are typically not detectable when the O I triplet is itself in absorption.

3.3 DV UMa (= US943)

Howell et al. (1988) classify this system as an SU UMa subtype because its orbital period is at the lower edge of the period gap (0.08597 d); however no superoutbursts or superhumps have yet been observed. This is an eclipsing system with depth of eclipse ~2 mag and a maximum *V* magnitude in quiescence of 18.6 (Szkody & Howell 1993). Both of the spectra shown in Fig. 1 are from the fourth night. Given the short orbital period and the long

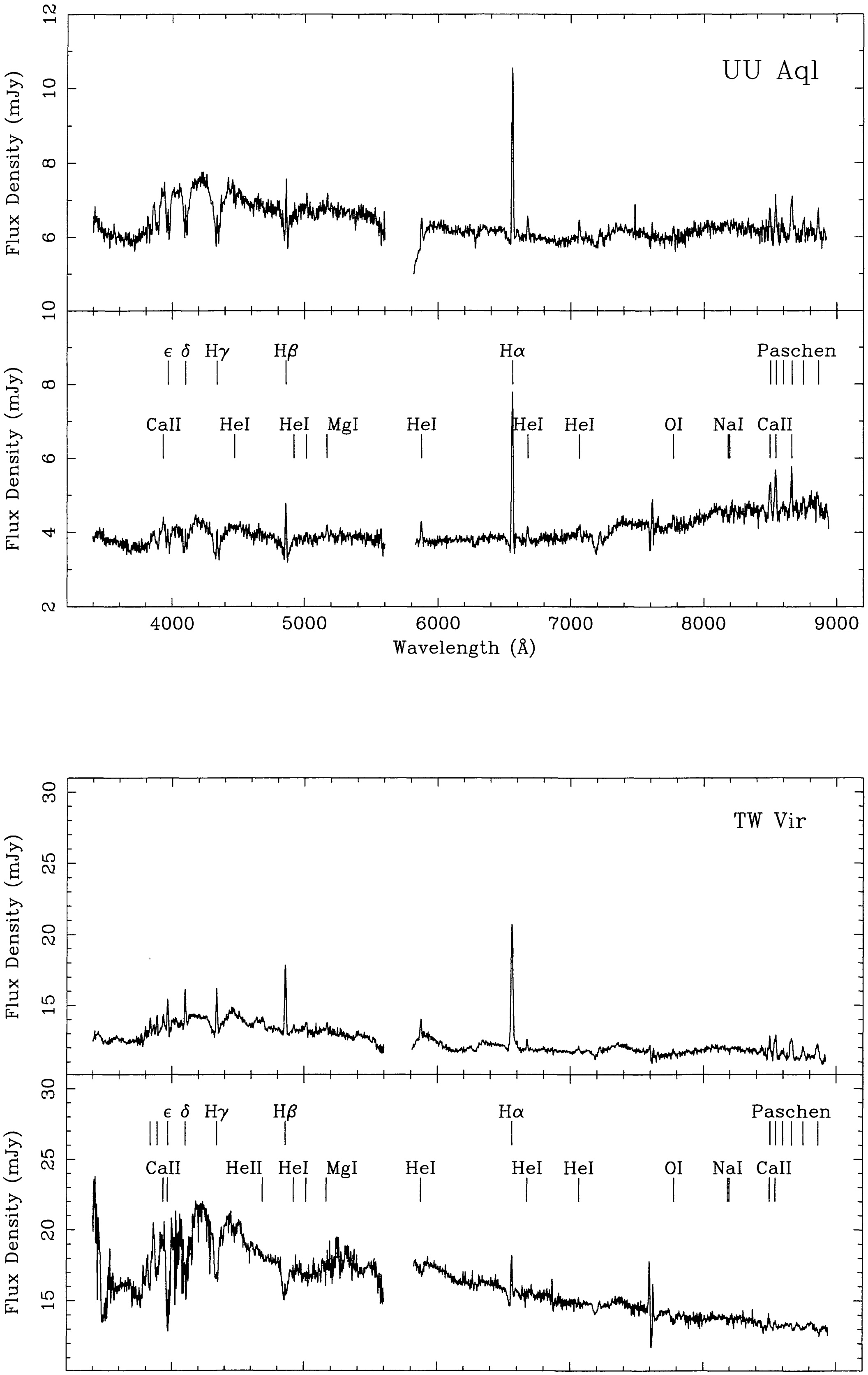

Figure 1. Spectra of UU Aql, TW Vir and DV UMa showing the significant variations in continuum level and line morphology. In the case of UU Aql and TW Vir the two panels correspond to spectra taken on different nights; the top panel showing a single spectrum taken on the first night in both cases, and the bottom panel showing an average of the spectra taken on night 2 for UU Aql and on night 4 for TW Vir. For DV UMa we show the two spectra taken on the same night. In all cases the Na I doublet at 8200 Å is just visible, as are several TiO band lines. See text for more comments.

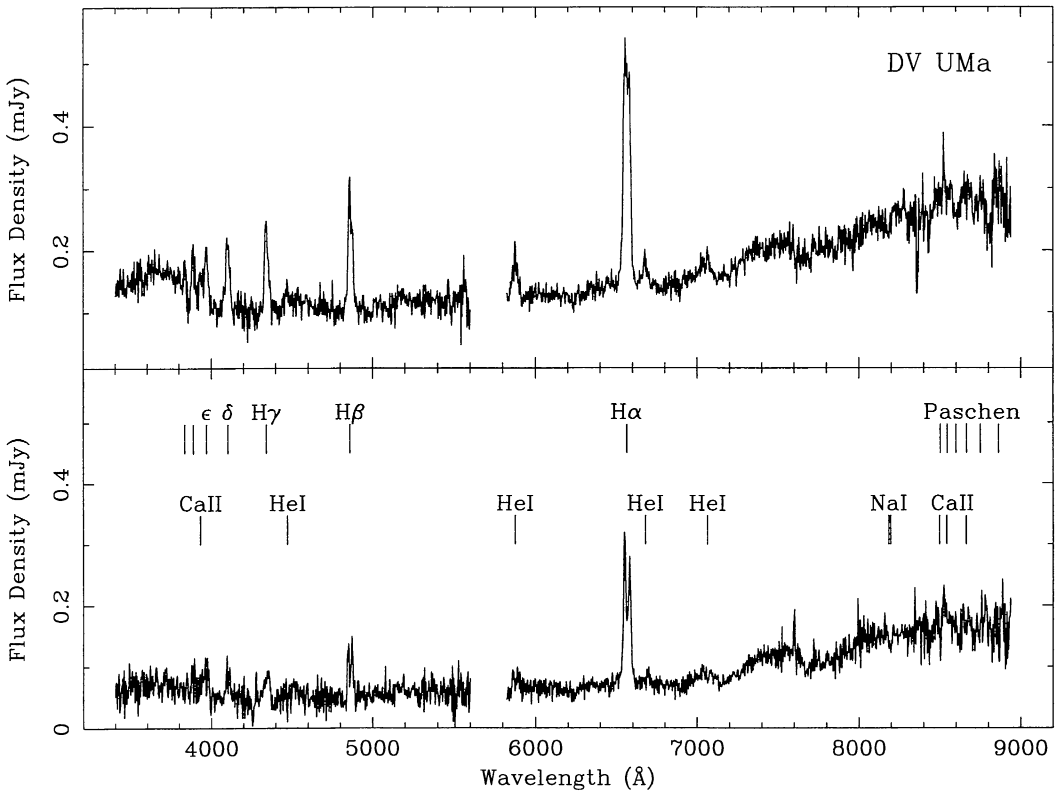

Figure 1 – *continued*

exposures, they are approximately 0.2 of a binary phase apart and the differences between them are easily discernible. Unfortunately, it is not possible for us to determine the exact binary phase of our observations because the high inaccuracies of the ephemeris found by Howell et al. (1988) are likely to yield incorrect eclipse times if extrapolated to 1991 (cf. Szkody & Howell 1993). The top spectrum clearly exhibits the higher Balmer lines and a good number of He I lines in emission, all of which have a double-peaked structure, more evident in the lower spectrum. Such line profiles are typical in high-inclination systems. Szkody & Howell (1993) arrived at a value for the inclination of 72° from their radial velocity study.

The red TiO bands, and possibly K I λλ7664-, 7698-Å lines in absorption, are detected as well as the Na I doublet. The infrared Ca II triplet is also in absorption; since the Balmer lines show no absorption components to suggest that the system has recently been in outburst, the Ca II triplet probably originates in the secondary. The TiO band ratio measurements of the individual spectra agree very well. Both result in a spectral type for the red dwarf in the range M4–5. This is an exceedingly good match to the spectral type of M4.5 suggested in Mukai et al. (1990). However, the contribution of the red dwarf to the total continuum flux is quite different from one spectrum to the next. In the first one (top panel in Fig. 1) it is about 36 per cent while in the second spectrum (bottom panel) we find a contribution of 60 per cent. The values quoted in Table 2 correspond to the average. So far there have only been two attempts to determine the parameters of DV UMa. Photometric data yield a mass estimate for the secondary of $0.17\,M_{\odot}$ (Howell & Blanton 1993) while the spectroscopic analysis by Szkody & Howell (1993) finds a slightly higher mass of $0.23\,M_{\odot}$.

3.4 Z Cam

The bright, well-studied system Z Cam was included in the survey for comparison purposes. As expected, our quiescence spectrum (Fig. 2) shows Balmer, Paschen and neutral He lines in emission, from the disc, and a very red continuum with clear Na D, Na I doublet at λ8190 Å and weak TiO absorption features, from the red star. There are also a number of other absorption features typical in late-K and early-M dwarfs. Indeed the secondary in this binary has been classified as a K7 dwarf by Wade (1981).

3.5 AT Cnc

This poorly studied system is described by Ritter & Kolb (1993) as being a dwarf nova of Z Cam type. Götz (1985, 1986) has reported photographic photometry and obtained a period of 5.7 h. The only previously published spectrum is a single low-resolution (18 Å) CCD spectrum taken as part of a new Asiago atlas (Zwitter & Munari 1994). Because of the low resolution, and the lack of correction for atmospheric absorption, that spectrum shows little other than Hα in emission plus a blue continuum. Two weak absorption features are probably Hβ and possibly NaD. Our five spectra (Fig. 2) show the Balmer lines in absorption, and a blue continuum which strengthens between night 2 (lower spectrum) and night 3 (upper spectrum), suggesting that the system was undergoing an outburst at the time. The night 3 data show the Na I doublet, and the Na D line is apparent in absorption on both nights. Since the Na D doublet is particularly prominent and the TiO bands are not visible, the secondary is likely to be a late-K or an early-M dwarf. Comparison of the red spectrum with our spectral-type standards yields a best match for spectral types in the range K7–M0. The red continuum has a broad hump; this is probably not a cyclotron hump, since no other component is evident and the hump is not quite broad enough (cf. the spectrum of AN UMa, in Section 5.3).

The Hα line is highly asymmetric, and appears to have a P Cygni profile, suggesting a disc wind.

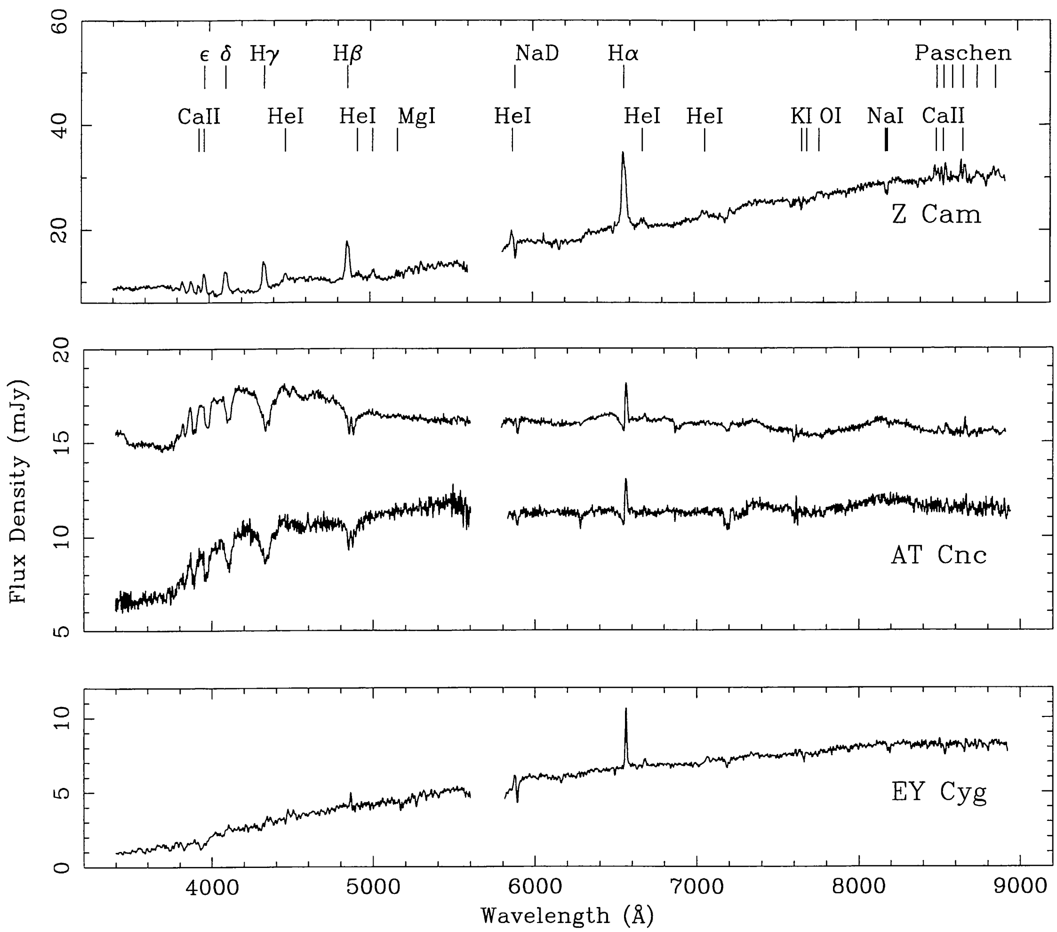

Figure 2. The spectra of Z Cam, AT Cnc and EY Cyg. The plots shown of Z Cam and EY Cyg correspond to a single spectrum while the ones of AT Cnc are an average of the existing spectra on each night. The lower spectrum is from night 2 and the upper one is from night 3. All three objects show a steep rise to the red, and there are several clear absorption lines from the red dwarf.

3.6 EY Cyg

EY Cyg is a U Gem-type dwarf nova with an outburst interval of about 240 d and outburst duration 30 d (Piening 1978). Its V magnitude in quiescence is 15.5. It has been detected by *ROSAT* in soft X-rays (0.4 to 2.2 keV) (Orio & Ögelman 1992), consistent with the observation by *HEAO-1* at energies above 0.48 keV (Córdova, Jensen & Nugent 1981).

Various attempts have been made in the past to measure the orbital period of EY Cyg. Using five photographic spectra, Kraft (1962) found that the lines showed no detectable velocity variations suggesting a long orbital period and/or a low-inclination system, although his detection limit was only about 70 km s^{-1}. Subsequent spectroscopic observations ($\lambda\lambda$ 4300–5000 Å) by Szkody, Piché & Feinswog (1990), taken 12 and 13 d after an outburst peak, gave further support to Kraft's (1962) findings. Again, the measured velocities for Hβ and Hγ were consistent with zero, but only two spectra were available. The photometric observations have been more successful in revealing the orbital period. Hacke & Andronov (1988) found a photometric period of 0.18 d, based on 281 photographic observations from Odessa and Sonneberg. However, their derived value had a high uncertainty because of the very large scatter in the data. Recently, a more reliable period of 0.2185 ± 0.0005 d has been determined by Sarna, Pych & Smith (1995), based on photoelectric data. Therefore the lack of detectable velocity shifts in the spectrum is more likely to be the result of a low inclination.

In our single spectrum (Fig. 2), the Balmer and He I emission lines are rather weak, and the continuum is very red, which suggests that the system was in a quiescent phase. There are many absorption features from the red dwarf component; these include the 5890-Å (Na D) and 8200-Å Na I doublets, possibly the K I line (λ 7698 Å), weak TiO bands redward of 7053 and 7666 Å and rather weak CN(1,2) (λ 4197 Å), CH(0,0) (λ 4314 Å) and CH(2,2) (λ 4324 Å) lines. Interestingly, the red Ca II triplet near 8500 Å appeared in absorption, suggesting that it may be from the red star rather than from the disc.

This is the first firm detection of the red component in this system since it was recognized as a CV, although Kraft (1962) reported a composite spectrum sdBe + K0V, and Antipova (1987) claimed evidence for a secondary without giving a reference. We compared the relative fluxes and depths of the Na D and Na I doublets with our M dwarf standard star spectra. From this we estimate the spectral type of the secondary to be K5–M0.

3.7 CG Dra

A brief discussion of what little is known about this U Gem-type dwarf nova is given by Bruch & Schimpke (1992). Our single spectrum (Fig. 3) resembles their spectrum in the region of overlap. Although the Na I doublet near 8200 Å is barely detectable, the Na D doublet near 5890 Å is a prominent absorption feature, along

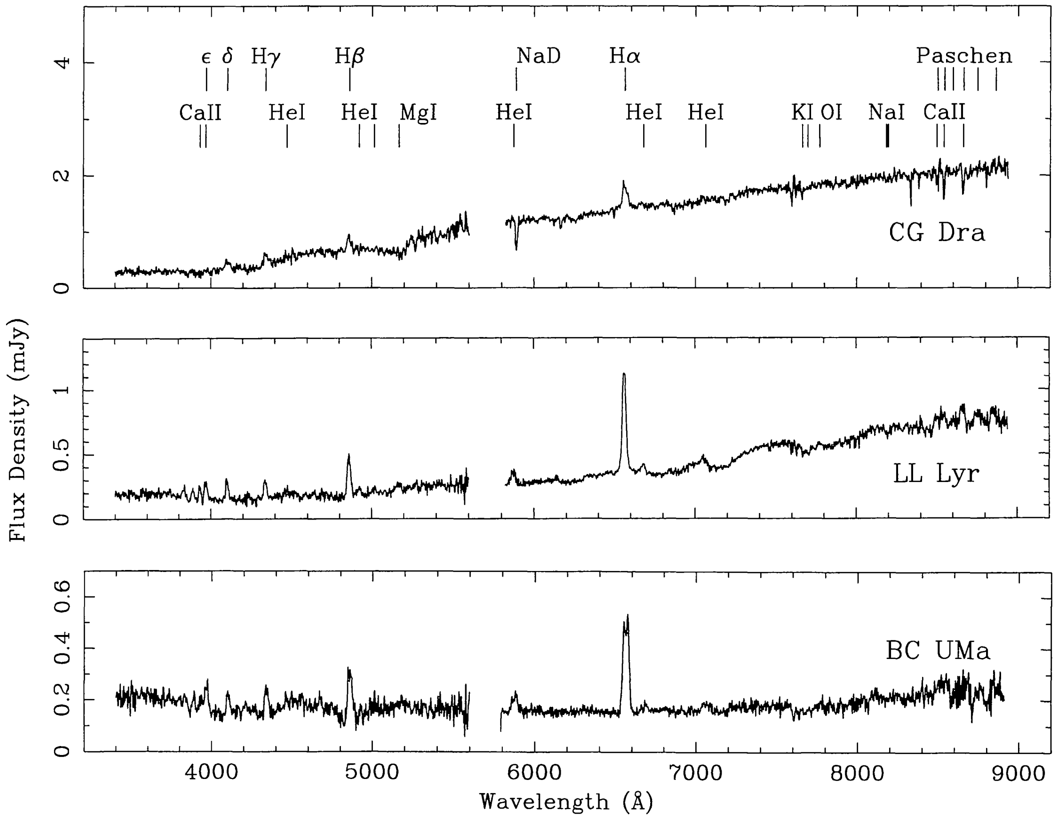

Figure 3. The spectra of CG Dra, LL Lyr and BC UMa. A single spectrum is shown for CG Dra and BC UMa. In the case of LL Lyr we give the average of the three spectra. CG Dra and LL Lyr show a particularly steep rise of the continuum level in the red with the TiO bands clearly showing in LL Lyr.

with the far-red Ca II triplet, also in absorption, indicating a late-type secondary. On the basis of the absorption-line spectrum, Bruch & Schimpke roughly classified the secondary as an early-K type. The weakness of the 8200-Å doublet in our spectrum confirms this suggestion. By the technique of spectral decomposition, Schimpke & Bruch (1992) have managed to narrow down the range to K5–M0 for the red dwarf in CG Dra.

Since the TiO bands are not prominent in K dwarfs it is not possible to employ the TiO ratio technique as we have done with the other systems in this survey. Instead we used the method by Ginestet et al. (1994) which is based on the strengths of the near-infrared spectral features and the ratios between them. The line equivalent widths were found to be strongly correlated with spectral type. In CG Dra, in addition to the Ca II triplet, other absorption lines such as Ti I λ8435 and Fe I λ8688 are clearly discernible in the spectrum. We measured the equivalent widths of these lines and used the relationships between Ca II and spectral type, Ti I and spectral type and the ratio Fe I λ8688/Ca II λ8542 and spectral type for main-sequence stars found by Ginestet et al. (see figs 8, 11 and 14 in Ginestet et al. 1994). We find that the cool component in CG Dra lies in the spectral-type range K5–7.

3.8 LL Lyr

According to Bruch & Schimpke (1992), LL Lyr was discovered as a Mira variable by Hoffmeister, who in a later publication revised the classification, assigning the star to the dwarf novae; it is given as UG in the General Catalogue of Variable Stars (GCVS: Kholopov 1985). The outbursts of LL Lyr repeat at intervals of 105–125 d. In quiescence, the *V* magnitude is about 17.1. No orbital period has been measured. The system has been detected in X-rays by *HEAO-1* (Córdova et al. 1981), although only at energies below 0.48 keV.

In the common range of wavelength (4000–7000 Å), our spectrum of LL Lyr (Fig. 3) is quite similar to the one shown by Bruch & Schimpke (1992). It is quite typical for a dwarf nova, with emission lines of H, He I, Fe II, O I and Ca II and a few Paschen lines. Schimpke & Bruch (1992) attempted a spectral decomposition, but were unable to put any constraint on the secondary star. However, in the red part of our spectrum we have very clear evidence for the red dwarf (TiO bands, Na I doublet and K I). Based on the TiO band flux ratios we derive a spectral type of M3–4 for the cool component.

The large contribution of the red star to the spectrum (~50 per cent) makes this system a prime target for mapping the secondary in search of irradiation effects (Davey & Smith 1992, 1996; Rutten & Dhillon 1994).

3.9 BC UMa

This dwarf nova has been observed over a similar wavelength range, at rather lower resolution, by Mukai et al. (1990), who note a strong resemblance to the spectrum (and orbital period) of WZ Sge and suggest a type of SU UMa rather than the U Gem classification given by the GCVS and Ritter & Kolb (1993). Recently, based on a collection of American Association for Variable Star Observers (AAVSO) data and their own photometric observations following a superoutburst, Howell et al. (1995) have confirmed the suggestion of Mukai et al. (1990). Howell et al. have also carried out *IUE* spectroscopic observations in the wavelength range λλ1150–3200 Å during outburst.

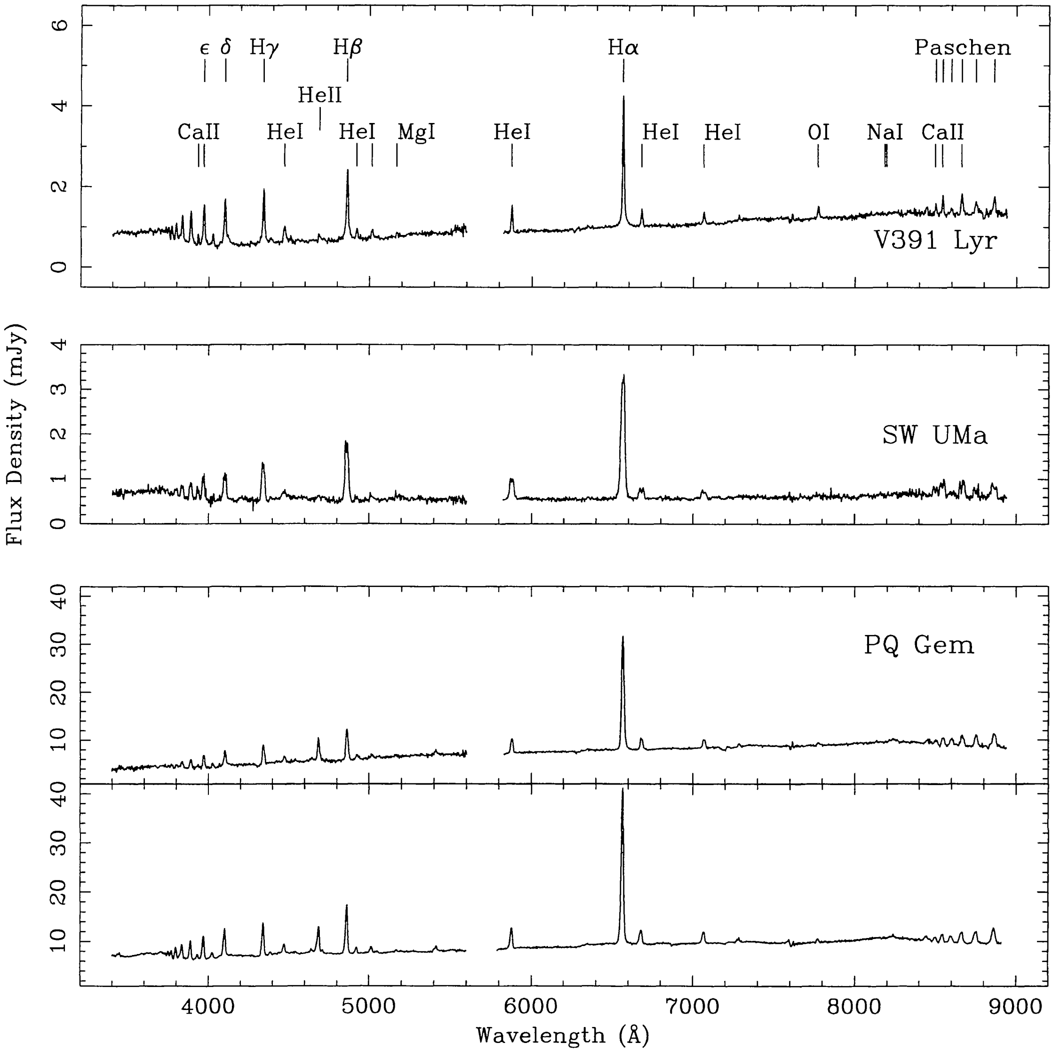

Figure 4. The spectra of V391 Lyr, SW UMa and PQ Gem (=RE J0751+144). With the exception of SW UMa, where we show a single spectrum, all the others are averages of the total collected for the object. In the case of PQ Gem the top panel is the average of the night 2 data and the lower panel that of night 3.

Our spectrum (Fig. 3), although noisy, confirms the general features found by Mukai et al. (1990): broad Balmer absorption lines with an emission core (dominant in Hα), and TiO bands in the red. With our higher resolution we are able to detect the TiO band at 7053 Å as well as that at 7666 Å. It is also just possible to detect the Na I doublet near 8200 Å, present in the model fitted by Mukai et al. (1990) but not visible in their spectrum. The TiO band ratio indicates a spectral type later than M5.

The emission cores are clearly double in our spectra, suggesting a relatively high inclination, although there is no evidence for an eclipse (Howell et al. 1990).

4 SYSTEMS THAT SHOW MARGINAL SECONDARY STAR SIGNATURES

There are three systems in our list for which we find a hint of the Na I doublet near λ8190 Å and in one case the TiO bands. However, because of the low signal-to-noise ratio and the weakness of the absorption features we are unable to ascertain the veracity of the detection. The systems are therefore not counted as detections for the statistics in Table 3 (later). In all cases the lines are well within the noise level, but they appear at the correct wavelengths within the errors.

4.1 V391 Lyr

As far as we are aware, the only other published spectrum of V391 Lyr is the one by Bruch & Schimpke (1992). Our spectrum (Fig. 4) is rather similar, showing a typical emission-line structure, but the lines are stronger and we covered a larger range of wavelength. Our spectrum was probably taken in quiescence. As well as the Balmer lines and a few Paschen lines, there are lines of He I, He II (λ4686 Å) and Ca II in emission. The O I triplet at 7773 Å is strongly in emission, which might have led us to expect an optically thin disc and some chance of seeing the secondary star (Friend et al. 1988). However, there are no totally convincing absorption lines in the spectrum, although there are hints of TiO bands and we have a marginal detection of the Na I far-red absorption doublet. The system is classified as Z Cam type in the GCVS.

4.2 SW UMa

Its orbital period of 82 min makes SW UMa one of the shortest-period SU UMa systems. Shafter, Szkody & Thorstensen (1986)

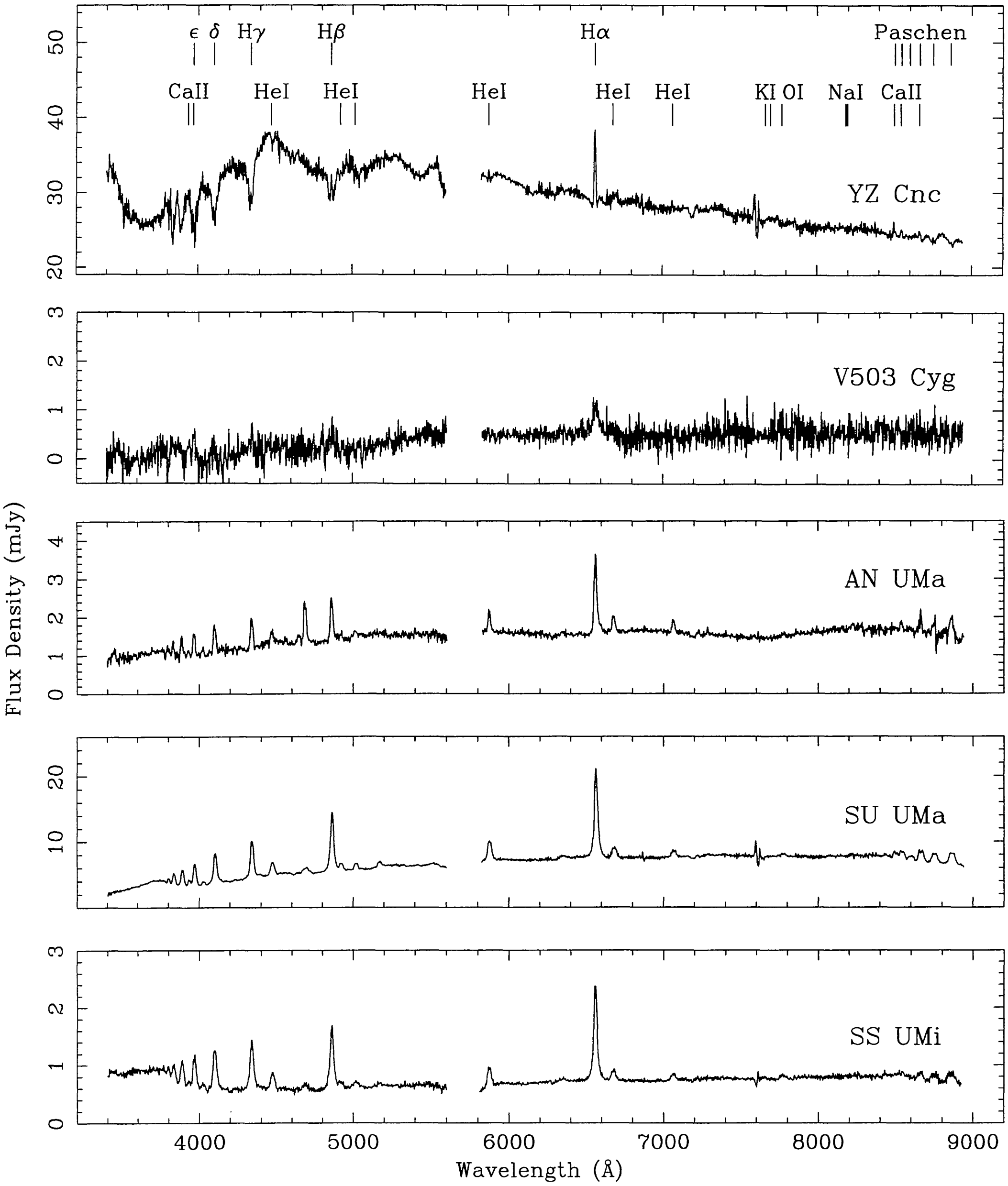

Figure 5. Average spectra of YZ Cnc, AN UMa, SU UMa and SS UMi, and a single spectrum of V503 Cyg. The spectrum of YZ Cnc shows strong absorption features which suggest that the system was undergoing an outburst. The unusual shape of the continuum in the blue may be the result of a calibration problem. The cyclotron humps are clearly visible in the red continuum of AN UMa.

found a period of about 16 min, which they interpreted as the white dwarf rotation period. If correct, this would make the system unique in being both an intermediate polar and a normal dwarf nova. However, Patterson (1994) also observed SW UMa and failed to find the 16-min period; he therefore rejected its classification as an IP/DQ Her star. SW UMa also exhibits quasi-periodic oscillations (QPOs) at shorter periods (Robinson et al. 1987; Kato, Hirata & Mineshige 1992).

Our spectrum (Fig. 4) shows only a very flat continuum and the usual hydrogen, helium and Ca II emission lines. The line profiles are perceptibly double although some of the lines show a much more complex structure. For example, the double peak clearly visible in the He I and Paschen lines in the red spectrum is not so obvious in the Hα line. Shafter et al. (1986) already noted that a narrow component, which cannot be attributed to the hotspot, is present in the emission features. Howell et al. (1995) have observed this object with *IUE* six days after a superoutburst and also found very complex line profiles. The double-peaked line structure suggests a fairly high-inclination system. However, Robinson et al. (1987) found $i = 44° \pm 18°$. It is thus a particularly interesting system, for which it would be very useful to constrain the dynamics by observing the motion of the red star.

Our only spectrum indicates the possible presence of the Na I absorption in the far-red. However, the detection is marginal and with only one spectrum it is difficult to ascertain whether or not it is a double-lined binary.

4.3 PQ Gem (=RE J0751+144)

As its original name indicates, the magnetic cataclysmic variable

RE J0751+144 (now PQ Gem) was discovered as an EUV source (Mason et al. 1992) during the *ROSAT* Wide Field Camera all-sky survey (Pounds et al. 1993) and was classified as an intermediate polar (IP). It is unusual in being the first IP to display EUV emission and in exhibiting elements of both the models that have been advanced to explain the spin modulation in IPs (Mason et al. 1992). It was also only the second IP to have circular polarization detected (Rosen, Mittaz & Hakala 1993; Piirola, Hakala & Coyne 1993). However, a recent study of the X-ray and *I*-band intensity variations by Väth, Chanmugam & Frank (1996) found that the magnetic field at the poles is likely to be in the range 9–12 MG, more typical of AM Her stars, and that accretion takes place on to a much smaller fraction of the white dwarf surface than is usual in IPs. This led them to describe it as an asynchronous AM Her rather than as an IP, although the distinction is arbitrary.

No orbital period has yet been found, but Rosen et al. (1993) and Hellier, Ramseyer & Jablonski (1994) used the spin and beat pulsations to deduce orbital periods of 5.3 and 5.2 h respectively, which would suggest a secondary of more than 0.5 $M_{\odot}$. We might expect to detect such a secondary easily if the disc is not too bright. As it turns out our spectra (Fig. 4) only show very weak indications of the red dwarf. The continuum is relatively flat. Nevertheless, we have a comparatively higher degree of confidence in the detection of the Na I doublet near λ8190 Å in this case than in the previous two objects because the average spectra from both nights exhibit the lines. Moreover, their measured fluxes are comparable, for example, to those in TW Vir, for which we have a firm detection. Unfortunately, the errors in this case are about 50 per cent. There is a strong He II emission feature at λ8237 Å which may be partially to blame.

Otherwise Fig. 4 shows a characteristic AM Her spectrum, with H I, He I, Ca II, He II and C III in emission. Also present is a weak O I emission line at λ7773 Å. The average spectrum from each night is plotted separately as there appears to be a slight change in the level of the continuum and the strengths of the low-excitation lines, the system being seemingly brighter on night 3; however, lack of spectrophotometry reduces the significance of this change.

5 THE OTHER SYSTEMS

Of the remaining six systems, the spectra of the nova-like BH Lyn have been published elsewhere (Dhillon et al. 1992); we present here spectra of the other five.

5.1 YZ Cnc

The SU UMa system YZ Cnc was included in the survey because it had been a prime target in the 1988 International Time Programme (ITP) on the Canary Island telescopes. The small number of red spectra taken on that programme suffered from a calibration problem, so we planned to use our ISIS spectra (Fig. 5) to supplement the ITP blue spectra and look for evidence for the red component.

In the event, it appears that our spectra were taken in outburst, since the Balmer lines are in absorption and the continuum is very blue. This is not surprising, because the interval between eruptions is known to be very short (about 10 d). Indeed that was the reason for putting it on the ITP target list, the aim of the ITP being to look at the behaviour of the system in different outburst phases (van Paradijs et al. 1994). Thus we are unable to add anything to the study by Shafter & Hessman (1988).

5.2 V503 Cyg

This SU UMa-type dwarf nova has only a few published spectra, the best low-dispersion spectrum being by Bruch & Schimpke (1992), who also give references to earlier publications. Our single spectrum (Fig. 5) was taken near dawn, and tracking was lost during the exposure. As a result, there were many night sky lines to remove, the spectrum is much noisier, and it shows little except Hα, Hβ and possibly Hγ. There is no sign of secondary star features, although infrared photometry (Szkody 1985) gives $V-J=2.7$ at minimum brightness. Szkody & Howell (1993) used Balmer-line radial velocities (Hβ, Hγ) to deduce a low mass for both stars, but the observations were complicated by uncertainties over the spectroscopic period, which appears to differ from the photometric one even in quiescence. In fact, three different periodicities have been detected in this system. A recent spectroscopic and photometric analysis during quiescence and through various outburst and superoutburst cycles by Harvey et al. (1995) found a spectroscopic period of 111.9 min, which they interpret as the binary orbital period, a periodic superoutburst signal at 116.7 min consistent with the presence of a superhump, and a large-amplitude wave with a period of 109.0 min which was present both during quiescence and during both short eruptions and superoutbursts, and which they refer to as the 'negative superhump'.

It would be useful to obtain infrared spectra of this object, to look for secondary star lines (Dhillon & Marsh 1993) and to obtain a better constraint on the dynamics.

5.3 AN UMa

Our spectrum of this magnetic system (Fig. 5) is similar to previously published spectra (e.g. Cropper et al. 1988) and clearly shows the cyclotron humps that enable the magnetic field (36 MG) to be estimated. Regarding the red dwarf, Voikhanskaya (1986) found no signs of it in the spectrum throughout a 5-night observing campaign in 1981 and 1983. Even during an unusually deep minimum, wherein the continuum was reported to have become very red, no absorption features of the secondary were seen. Although we have looked further into the red region than Voikhanskaya (1986), we obtain the same negative result. Despite the lack of a disc there is no obvious sign of the secondary star in our spectrum. We believe the strong He II line at λ8237 Å may be partially contaminating the region near the Na I doublet, adding difficulty to the detection of the red dwarf.

5.4 SU UMa

Like YZ Cnc, SU UMa was a prime target in the 1988 International Time Programme (ITP) (van Paradijs et al. 1994) and was placed on our observing list for the same reason. On this occasion, we appear to have caught the star in quiescence and the blue spectrum is similar to those published by Thorstensen, Wade & Oke (1986), by Szkody (1987) and by the ITP team (Rutten, van Paradijs & Tinbergen 1992). We are not aware of a previously published red spectrum, although Thorstensen et al. (1986) observed SU UMa in the range 5800–7200 Å and published the Hα profiles.

Our average spectrum (Fig. 5) shows no sign of any secondary star features, as is typical in the short-period systems whose secondaries are expected to be of low mass and therefore very faint. Interestingly, there is a great deal of structure in the emission lines. There is some hint of line-doubling in the Paschen and He I lines, although the Balmer lines appear to be single. In particular,

Table 3. The number of systems of different type that show spectroscopic features of a secondary star. EI UMa and V589 Her have been excluded from the statistical analysis.

Type of system	Number	Secondary detected	Percentage of total
DN/ZC	3	2	66
DN/UG	5	5	100
DN/SU	6	1	16
DN/UG or SU	1	1	100
All DN	15	9	60
AM	1	0	0
IP	1	0	0
NL	1	0	0
DS	2	2	100
Total	20	11	55

the He I emission lines exhibit flat peaks which sometimes have a very sharp and narrow emission core. A complex emission-line structure was found by Thorstensen et al. (1986) in the Hα profiles which we do not detect in our data set perhaps due to the low resolution of our spectra. The O I line at λ7773 Å is in emission in our spectrum.

5.5 SS UMi = PG 1551+719

The nature and orbital period of this PG object (Green et al. 1982) were uncertain until fairly recently. Photometry in outburst by Chen, Liu & Wei (1991) showed humps with a separation of 101 min on three different nights, while no such humps were observed in quiescence. This led them to classify the system as an SU UMa, and to deduce an orbital period of 98 min, although at the time there was no direct evidence for this. Photometric and time-resolved spectroscopic observations by Thorstensen et al. (1996) have now confirmed this value. They measure an orbital period of 97.6 min.

Our spectrum (Fig. 5) is consistent with the quiescence spectra obtained by Mason et al. (1982) in their discovery paper and that shown by Thorstensen et al. (1996). The continuum is fairly flat, giving no hint of a secondary star contribution. H I, He I, He II and O I are all found in emission. As with SU UMa, the He I lines show a complex structure as opposed to the Balmer lines which are sharply single-peaked. In the spectrum published in Thorstensen et al. (1996) the He I emission lines actually appear double-peaked.

6 OVERALL STATISTICS

The statistics are summarized in Table 3. As mentioned earlier, EI UMa and V589 Her have been excluded from the analysis because of possible misidentifications.

The most obvious result is the surprisingly high fraction of systems in which the secondary was detected, much higher than the 25 per cent uncovered in the previous survey. However, there is a considerable selection effect. Z Cam was included as a comparison system, RE J1629+780, a *ROSAT* source, was observed because of its reportedly interesting spectrum, NN Ser was known to be a detached system and was observed as a suspected pre-cataclysmic variable and two systems, BC UMa and DV UMa, were already known to show secondary star features from the paper by Mukai et al. (1990). If these systems are removed, the fraction drops to 6 out of 15, or 40 per cent. Even so, this is two more systems than the four that would have been expected from the fraction found in the previous survey, and this is without taking into account the three systems for which we suspect a detection of the secondary star.

One factor is that the S/N ratio was higher for most of the spectra in the present survey. However, it is also true that the original list was chosen to include systems for which the red star might be expected to be detectable, since one purpose of the survey was to find more systems in which properties of the secondary could be measured directly. We selected systems that were in the 'inconclusive' category in the previous survey, together with various unpublished 'inconclusives' and 'hopefuls' observed between the first survey and the second one. Because of the poor seeing, we concentrated on the brighter objects in our list, which tended to mean the longer period objects, in which it was more likely that the secondary would be detected. The high discovery rate is therefore partly just a reflection of a successful search strategy.

As one would expect, it is easier to detect the secondary in dwarf novae and detached systems than in nova-likes with larger mass transfer rates. A larger sample of magnetic systems will need to be gathered before any conclusions can be drawn about why the secondary is visible in some systems and not in others of a similar period. The detection of the secondary in QQ Vul (Mukai & Charles 1986, 1987) and in AM Her (Young & Schneider 1981), with periods of 3.71 and 3.09 h respectively, and correspondingly more massive secondaries, is not surprising; however, the secondary has also been detected in ST LMi and MR Ser (Mukai & Charles 1986, 1987), whose periods of 1.90 and 1.89 h are similar to that of AN UMa (1.91 h). The most likely explanation is that the visibility of the secondary is related to whether or not the system has a high mass transfer rate either as a result of a temporary increase, such as during a high state, or simply because it is its normal state.

7 CONCLUSIONS

This survey has uncovered the red dwarfs in a number of particularly interesting new systems, with a discovery fraction of secondary stars more than 50 per cent larger than that of our previous survey. We have detected the red dwarf star in the faint cataclysmic variables UU Aql, AT Cnc, EY Cyg, CG Dra, LL Lyr, BC UMa, DV UMa and TW Vir, as well as in Z Cam, and in the detached systems NN Ser and RE J1629+780. We have derived the spectral type of the secondary in the eight faint semi-detached binaries listed above. In addition, marginal signs of the secondary in V391 Lyr, SW UMa and PQ Gem have been found. Unfortunately, with the limited number of spectra we are unable to ascertain the significance of the detection.

The secondary has been detected in almost all the dwarf novae and other semi-detached systems with periods above the gap. The exceptions are BH Lyn, which is a nova-like with a prominent disc, and a marginal detection of the secondary in PQ Gem, which may have a disc. This may suggest that the two systems with detected secondaries but without known periods (CG Dra and LL Lyr) have periods above the gap. This is consistent with our derived spectral types for the secondary star in these systems.

ACKNOWLEDGMENTS

This work was supported in part by the Polish National Committee for Scientific Research under grant 2–2115–92–03 and in part by the SERC PATT under rolling grant GR/G 51473. The data reduction and analysis were carried out on the Microvax 3400 and

Vaxstation 3100 system at the Sussex node, and SunSolaris systems at the Sussex and St Andrews nodes, of the SERC/PPARC Starlink Project. The William Herschel Telescope is operated by the Royal Greenwich Observatory at the Observatorio del Roque de los Muchachos of the Instituto de Astrofísica de Canarias. We thank Vik Dhillon for preliminary reduction of the red spectra of 17 of our targets and for comments on the manuscript.

REFERENCES

Andronov I. L., Shakun L. I., 1990, Ap&SS, 169, 237

Antipova L. I., 1987, Ap&SS, 131, 453

Bianchini A., 1990, AJ, 99, 1941

Bruch A., Schimpke T., 1992, A&AS, 93, 419

Catalán M. S., Davey S. C., Sarna M. J., Smith R. C., Wood J. H., 1994, MNRAS, 269, 879

Catalán M.S., Sarna M. J., Jomaron C. M., Smith R. C., 1995, MNRAS, 275, 153

Chen J.-S., Liu X.-W., Wei M.-Z., 1991, A&A, 242, 397

Cooke B. A. et al., 1992, Nat, 355, 61

Córdova F. A., Jensen K. A., Nugent J. J., 1981, MNRAS, 196, 1

Cropper M. S. et al., 1988, MNRAS, 236, 29P

Davey S. C., Smith R. C., 1992, MNRAS, 257, 476

Davey S. C., Smith R. C., 1996, MNRAS, 280, 481

Dhillon V. S., Marsh T. R., 1993, Ann. Isr. Phys. Soc., 10, 34

Dhillon V., Jones D. H. P., Marsh T. R., Smith R. C., 1992, MNRAS, 258, 225

Friend M. T., Martin J. S., Smith R. C., Jones D. H. P., 1988, MNRAS, 233, 451

Ginestet N., Carquillat M., Jaschek M., Jaschek C., 1994, A&AS, 108, 359

Götz W., 1985, Inf. Bull. Variable Stars, 2734

Götz W., 1986, Inf. Bull. Variable Stars, 2918

Green R. F., Ferguson D. H., Liebert J., Schmidt M., 1982, PASP, 94, 560

Hacke G., Andronov I. L., 1988, Mitt. Ver. Sterne, 11(4), 74

Harvey D., Skillman D. R., Patterson J., Ringwald F. A., 1995, PASP, 107, 551

Hellier C., Ramseyer T. F., Jablonski F. J., 1994, MNRAS, 271, L25

Horne K., 1986, PASP, 98, 609

Howell S. B., Blanton S. A., 1993, AJ, 106, 311

Howell S. B., Mason K. O., Reichert G. A., Warnock A., Kreidl T. J., 1988, MNRAS, 233, 79

Howell S. B., Szkody P., Kreidl T. J., Mason K. O., Puchnarewicz E. M., 1990, PASP, 102, 758

Howell S. B., Szkody P., Sonneborn G., Fried R., Mattei J., Oliversen R. J., Ingram D., Hurst G. M., 1995, ApJ, 453, 454

Kato T., Hirata R., Mineshige S., 1992, PASJ, 44, L215

Kholopov P. N., ed., 1985, General Catalogue of Variable Stars, 4th edn. 'Nauka' Publishing House, Moscow (GCVS)

Kirkpatrick J. D., Henry T. J., McCarthy D. W., Jr, 1991, ApJS, 77, 417

Kraft R. P., 1962, ApJ, 135, 408

Mansperger C. S., Kaitchuck R. H., 1990, ApJ, 358, 268

Martin J. S., Friend M. T., Smith R. C., Jones, D. H. P., 1989, MNRAS, 240, 519

Mason K. O., Reichert G. A., Bowyer S., Thorstensen J. R., 1982, PASP, 94, 521

Mason K. O. et al., 1992, MNRAS, 258, 749

Mateo M., Szkody P., Bolte M., 1985, PASP, 94, 45

Mukai K., Charles P. A., 1986, MNRAS, 222, 1P

Mukai K., Charles P. A., 1987, MNRAS, 226, 209

Mukai K. et al., 1990, MNRAS, 245, 385

Oke J. B., Gunn J. E., 1983, ApJ, 266, 713

Orio M., Ögelman H., 1992, IAU Circ. 5680

Patterson J., 1994, PASP, 106, 209

Piening A. T., 1978 J. Am. Assoc.Variable Star Observers, 6, 60

Piirola V., Hakala P., Coyne G. V., S. J., 1993, ApJ, 410, L107

Pounds K. A. et al., 1993, MNRAS, 260, 77

Richman H. R., Applegate J. H., Patterson J., 1994, PASP, 106, 1075

Ritter H., 1990, A&AS, 85, 1179

Ritter H., Kolb U., 1995, in Lewin W. H. G., van Paradijs J., van den Heuvel E. P. J., eds, X-ray Binaries. Cambridge Univ. Press, Cambridge, p. 578 (circulated in 1993 as Garching preprint MPA 757)

Robinson E. L., Shafter A. W., Hill J. A., Wood M. A., Mattei J. A., 1987, ApJ, 313, 772

Rosen S. R., Mittaz J. P. D., Hakala P. J., 1993, MNRAS, 264, 171

Rutten R. G. M., Dhillon V. S., 1994, A&A, 288, 773

Rutten R. G. M., van Paradijs J., Tinbergen J., 1992, A&A, 260, 213

Sarna M. J., Pych W., Smith R. C., 1995, Inf. Bull. Variable Stars, 4165

Schimpke T., Bruch A., 1992, A&A, 266, 225

Shafter A. W., 1992, ApJ, 394, 268

Shafter A. W., Hessman F. V., 1988, AJ, 95, 178

Shafter A. W., Szkody P., Thorstensen J. R., 1986, ApJ, 308, 765

Smith R. C., Sarna M. J., Jones D. H. P., 1995, in Bianchini A., Della Valle M., Orio M., eds, Cataclysmic Variables. Kluwer, Dordrecht, p. 115

Szkody P., 1985, AJ, 90, 1837

Szkody P., 1987, ApJS, 63, 685

Szkody P., Howell S. B., 1993, ApJ, 403, 743

Szkody P., Piché F., Feinswog L., 1990, ApJS, 73, 441

Thorstensen J. R., Wade R. A., Oke J. B., 1986, ApJ, 309, 721

Thorstensen J. R., Patterson J. O., Shambrook A., Thomas G., 1996, PASP, 108, 73

van Paradijs J. et al., 1994, MNRAS, 267, 465

Väth H., Chanmugam G., Frank J., 1996, ApJ, 457, 407

Voikhanskaya N. F., 1986, AZh, 63, 516

Wade R. A., 1981, PhD thesis, California Institute of Technology

Wade R. A., Horne K., 1988, ApJ, 324, 411

Young P., Schneider D. P., 1981, ApJ, 247, 960

Zwitter T., Munari U., 1994, A&AS, 107, 503

APPENDIX A: LIST OF IDENTIFIED LINES AND THEIR EQUIVALENT WIDTHS

In the following table we provide a list of the lines found in the spectra of the objects included in the survey, together with their equivalent widths and flux values. Although more than one spectrum was collected for most of the targets, for the majority hardly any changes in continuum level and in line flux were observed. For these objects we used the averaged spectra to measure the line strengths. However, for a few objects, significant changes were seen throughout the run, in some cases from one night to the next, and in others from one spectrum to the next. In order to show the magnitude of such variations, separate measurements are given. The column marked with an 'N' indicates the night the spectrum or spectra were observed following the same convention as in the main text, and the comments in the last column indicate whether the spectra were individually analysed (single spectrum) or whether an average was used.

Negative values of equivalent width correspond to emission lines, and positive ones represent absorption lines. The contrary rule applies for the flux values, in other words, positive measurements represent emission lines and negative ones absorption features. The fluxes were determined by fitting a Gaussian to the line profile and measuring the flux between the fitted profile and the continuum.

The measurements were fairly straightforward except for the few cases where the lines are composed of superimposed absorption and emission components or where a double-peaked structure is present. Where both emission and absorption components are present, and clearly distinct, these were fitted separately. Thus two values are quoted for one particular line. Otherwise, only the more visible component is given, although in these cases the values are likely to be the sum of the two. Double-peaked features were fitted with two

Table A1. Fluxes and equivalent widths of the lines found in the spectra of the survey targets.

	Line species																				N	Comm.
	HI										HI											
	Hα 6562		Hβ 4861		Hγ 4340		Hδ 4104		Hϵ 3970		P_{11} 8545		P_{10} 8598		P_9 8665		P_8 8750		P_7 8862			
Object	*f*	EW	*f*	EW	*f*	EW	*f*	EW	*f*	EW	*f*	EW	*f*	EW	*f*	EW	*f*	EW	*f*	EW		
UU Aql	0.43	−9.97	0.26	−3.57	–	–	–	–	–	–	–	–	–	–	–	–	0.02	−1.00	0.03	−1.25	1	Em.
	–	–	−1.37	5.18	−1.83	15.35	−1.00	7.29	−0.78	5.29	–	–	–	–	–	–	–	–	–	–	1	Abs.
	0.44	−12.53	0.11	4.42	−1.43	17.48	−0.63	6.97	−0.59	5.33	–	–	0.03	−4.82	–	–	–	–	–	–	2	Sp. 2
Z Cam	3.34	−32.66	2.81	−22.07	2.44	−17.41	2.38	−20.99	1.37	−13.60	–	–	–	–	–	–	0.11	−0.92	–	–	1	Sing. sp.
YZ Cnc	0.76	−2.53	−1.75	3.88	−5.90	11.30	−3.99	7.09	−3.92	6.63	–	–	–	–	–	–	−0.15	1.47	−0.19	1.84	4	Aver.
AT Cnc	0.17	−2.09	−0.41	5.81	−1.42	16.76	−0.54	6.17	–	–	–	–	–	–	–	–	–	–	–	–	2	Aver.
	0.17	−1.88	−1.08	7.84	−2.55	12.43	−1.01	4.35	−0.84	3.49	–	–	–	–	–	–	–	–	–	–	3	Aver.
EY Cyg	0.34	−8.16	0.10	−1.50	0.09	−1.84	0.14	−0.94	–	–	–	–	–	–	–	–	–	–	–	–	1	Sing. sp.
V503 Cyg	0.23	−72.20	0.20	−87.91	0.10	−68.34	–	–	–	–	–	–	–	–	–	–	–	–	–	–	2	Sing. Sp.
CG Dra	0.13	−14.24	0.07	−7.08	0.08	−9.69	0.09	−15.62	–	–	–	–	–	–	–	–	–	–	–	–	4	Sing. sp.
PQ Gem	3.13	−58.68	0.71	−21.26	0.48	−9.27	0.47	−13.83	0.38	−12.11	0.11	−2.64	0.10	−2.72	0.18	−5.05	0.19	−5.56	0.29	−9.12	2	Aver.
(= RE J0751+144)	11.24	−55.86	2.06	−21.93	1.52	−13.43	1.51	−12.53	1.46	−14.66	0.37	−5.96	0.36	−2.62	0.63	−4.80	0.75	−6.11	0.87	−7.12	3	Aver.
LL Lyr	0.15	−59.45	0.09	−36.82	0.06	−21.02	0.06	−22.03	0.04	−11.35	–	–	–	–	–	–	–	–	–	–	4	Sp. 1
	0.21	−79.48	0.12	−39.83	0.07	−22.60	0.08	−26.86	0.06	−27.73	–	–	–	–	0.03	−7.30	0.02	−5.10	0.01	−2.42	4	Sp. 2
	0.12	−68.92	0.07	−45.90	0.02	−10.03	0.03	−24.19	–	–	–	–	–	–	–	–	–	–	–	–	4	Sp. 3
V 391 Lyr	0.29	−51.69	0.31	−42.44	0.31	−42.33	0.34	−50.02	0.24	−22.75	0.02	−3.30	0.01	−1.40	0.03	−5.36	0.03	−5.66	0.03	−5.63	4	Aver.
SU UMa	2.64	−62.38	3.06	−45.52	2.45	−37.77	2.19	−36.24	1.45	−22.14	–	–	0.10	−3.21	0.25	−8.52	0.22	−7.99	0.29	−11.35	4	Aver.
SW UMa	0.58	−150.45	0.45	−72.30	0.29	−31.49	0.24	−24.85	0.21	−20.85	0.04	−12.30	0.01	−4.76	0.46	−16.19	0.03	−8.46	0.04	−16.45	4	Sing. sp.
AN UMa	0.41	−38.02	0.36	−17.69	0.31	−9.83	0.30	−12.69	0.24	−7.15	–	–	–	–	0.05	−6.79	0.04	−5.23	0.06	−10.53	2	Sp. 1
	0.24	−27.72	0.23	−19.29	0.16	−10.61	0.18	−13.20	0.15	−12.18	–	–	–	–	0.02	−1.87	0.01	−3.15	0.04	−6.92	2	Sp. 3
BC UMa	0.14	−97.78	0.08	−30.64	0.04	−9.57	0.04	−7.33	0.04	−10.39	–	–	–	–	–	–	–	–	–	–	3	Sp. 1
	0.08	−91.49	0.03	−20.41	0.02	−9.97	–	–	–	–	–	–	–	–	–	–	–	–	–	–	3	Sp. 2
DV UMa	0.13	−144.60	0.08	−72.35	0.06	−42.68	0.06	−32.25	0.04	−15.64	–	–	–	–	–	–	–	–	–	–	4	Sp. 1
	0.06	−123.95	0.03	−49.88	–	–	–	–	–	–	–	–	–	–	–	–	–	–	–	–	4	Sp. 2
SS UMi	0.33	−83.13	0.42	−67.86	0.37	−42.24	0.35	−33.66	0.27	−23.55	–	–	–	–	–	–	0.02	−5.59	0.04	−15.56	1	Aver.
TW Vir	1.06	−12.99	0.75	−4.09	0.59	−2.60	0.39	−1.25	–	–	–	–	0.01	−0.50	–	–	0.06	−1.30	0.11	−2.65	1	Sing. sp.
	0.19	−1.14	−1.18	5.09	−4.31	13.40	−4.53	9.57	−3.13	7.95	–	–	–	–	−0.03	0.47	−0.05	0.96	–	–	4	Aver.

Table A1 – *continued*

	Line species																		N	Comm.
	He I														He II					
	4026		4471		4922		5015		5875		6678		7065		4686		8237			
Object	*f*	EW	*f*	EW	*f*	EW	*f*	EW	*f*	EW	*f*	EW	*f*	EW	*f*	EW	*f*	EW		
UU Aql	–	–	–	–	–	–	0.05	−0.75	–	–	0.05	−1.06	0.04	−1.39	–	–	–	–	1	Sing. sp.
	–	–	–	–	–	–	–	–	0.06	−1.32	0.03	−0.60	–	–	–	–	–	–	2	Sp. 2
Z Cam	0.19	−1.43	0.51	−3.47	0.13	−1.04	0.48	−3.93	0.33	−2.25	0.49	3.61	0.24	−1.64	–	–	–	–	1	Sing. sp.
YZ Cnc	–	–	−0.19	0.27	−0.34	0.62	−0.11	0.38	−0.24	0.90	–	–	–	–	–	–	–	–	4	Aver.
AT Cnc	–	–	−0.19	0.90	–	–	–	–	–	–	0.04	−0.59	–	–	–	–	–	–	3	Aver.
EY Cyg	–	–	0.14	−3.10	–	–	–	–	0.09	−1.75	0.05	−0.99	–	–	–	–	–	–	1	Sing. sp.
V503 Cyg	–	–	–	–	–	–	–	–	–	–	–	–	–	–	–	–	–	–		
CG Dra	–	–	–	–	–	–	–	–	–	–	–	–	–	–	–	–	–	–		
PQ Gem	0.09	−1.88	0.16	−3.88	0.09	−2.36	0.07	−2.34	0.46	−7.40	0.30	−5.40	0.23	−4.47	0.48	−16.56	0.17	−2.46	2	Aver.
(= RE J0751+144)	0.47	−4.14	0.53	−5.05	0.21	−2.13	0.26	−3.41	1.85	−7.67	1.17	−5.67	0.80	−4.14	1.26	−16.14	0.21	−1.41	3	Aver.
LL Lyr	0.02	−4.08	–	–	0.02	−7.53	0.02	−9.09	0.03	−10.72	0.01	−4.52	–	–	–	–	–	–	4	Sp. 1
	–	–	–	–	–	–	–	–	0.04	−15.22	0.02	−8.46	–	–	–	–	–	–	4	Sp. 2
	–	–	–	–	–	–	–	–	0.02	−10.95	0.01	−3.80	–	–	–	–	–	–	4	Sp. 3
V 391 Lyr	0.05	−5.28	0.11	−13.31	0.04	−5.70	0.03	−4.41	0.06	−8.44	0.03	−5.18	0.02	−2.58	0.03	−3.86	–	–	4	Aver.
SU UMa	0.16	−2.24	0.97	−14.12	0.40	−5.21	0.26	−3.58	0.82	−13.64	0.35	−6.85	0.18	−3.78	0.34	−3.70	–	–	4	Aver.
SW UMa	–	–	0.05	−6.32	0.04	−6.14	0.03	−4.75	0.12	−24.88	0.05	−13.11	0.03	−8.46	0.04	−4.99	–	–	4	Sing. sp.
AN UMa	0.05	−1.86	0.17	−7.48	0.03	−1.57	0.05	−2.36	0.11	−7.15	0.08	−8.17	0.05	−4.80	0.33	−16.80	0.02	−2.90	2	Sp. 1
	–	–	–	–	–	–	–	–	0.07	−6.22	0.05	−5.95	0.03	−3.01	0.27	−20.06	–	–	2	Sp. 3
BC UMa	–	–	–	–	–	–	–	–	0.03	−16.67	–	–	–	–	–	–	–	–	3	Sp. 1
	–	–	–	–	–	–	–	–	0.01	−7.67	–	–	–	–	–	–	–	–	3	Sp. 2
DV UMa	–	–	0.02	−10.25	–	–	–	–	0.02	−16.96	0.01	−9.54	0.01	−3.11	–	–	–	–	4	Sp. 1
	–	–	–	–	–	–	–	–	0.01	−18.30	0.01	−13.08	–	–	–	–	–	–	4	Sp. 2
SS UMi	0.05	−3.94	0.12	−13.24	0.08	−9.14	0.06	−8.49	0.07	−11.34	0.04	−8.84	0.02	−3.92	0.04	−4.97	–	–	1	Aver.
TW Vir	–	–	–	–	0.06	−0.27	0.11	−0.70	0.14	−1.43	0.04	−0.43	0.03	−0.46	0.38	−1.47	–	–	1	Sing. sp.
	–	–	−0.89	2.11	–	–	−0.29	1.82	–	–	–	–	–	–	–	–	–	–	4	Aver.

Table A1 – *continued*

	Line species																				N	Comm.
	C III/N III		O I		Na I				Ca II													
	4640/4650		7773		5889/5895		8183/8194		3933		3968		8498		8542		8662					
Object	f	EW	f	EW	f	EW	f	EW	f	EW	f	EW	f	EW	f	EW	f	EW				
UU Aql	–	–	0.017	−0.37	–	–	−0.005	0.20	–	–	–	–	0.032	−1.16	0.051	−2.03	0.077	−3.48			1	Sp. 2
	0.026	−0.42	0.030	−1.14	–	–	−0.033	1.11	–	–	–	–	0.064	−2.67	0.092	−6.23	0.104	−4.82			2	Sing. sp.
Z Cam	–	–	–	–	−0.335	2.25	−0.175	1.35	0.287	−1.60	–	–	–	–	–	–	–	–			1	Sing. sp.
YZ Cnc	0.094	−0.22	–	–	–	–	–	–	–	–	–	–	0.047	−0.62	–	–	0.073	−0.73			4	Aver.
AT Cnc	–	–	–	–	−0.084	0.86	–	–	–	–	–	–	–	–	–	–	–	–			2	Aver.
	–	–	–	–	−0.095	1.00	−0.030	0.54	–	–	–	–	0.022	−0.51	0.048	−1.63	0.032	−0.79			3	Aver.
EY Cyg	–	–	–	–	−0.120	2.44	−0.051	1.62	−0.347	9.39	–	–	–	–	–	–	–	–			1	Sing. sp.
V503 Cyg	–	–	–	–	–	–	–	–	–	–	–	–	–	–	–	–	–	–			2	Sing. sp.
CG Dra	–	–	–	–	−0.058	5.11	−0.009	1.60	–	–	–	–	−0.006	1.08	−0.018	2.05	−0.017	1.67			4	Sing. sp.
PQ Gem	0.122	−3.07	0.054	−1.27	–	–	−0.011	0.20	0.096	−2.21	–	–	–	–	–	–	–	–			2	Aver
(= RE J0751+144)	0.269	−2.55	0.185	−1.16	–	–	−0.029	0.45	0.287	−2.45	–	–	–	–	–	–	–	–			3	Aver
LL Lyr	0.009	−3.00	–	–	–	–	−0.008	2.50	0.026	−20.86	–	–	–	–	–	–	–	–			4	Sp. 1
	–	–	–	–	–	–	−0.011	2.85	0.027	−6.15	–	–	0.024	−4.77	0.032	−6.83	–	–			4	Sp. 2
	0.021	−12.04	–	–	–	–	−0.003	0.84	–	–	–	–	–	–	–	–	–	–			4	Sp. 3
V391 Lyr	–	–	0.016	−2.23	–	–	−0.003	0.48	0.026	−1.81	–	–	–	–	–	–	–	–			4	Aver
SU UMa	0.189	−2.22	0.075	−1.96	–	–	–	–	0.308	−4.26	–	–	–	–	–	–	–	–			4	Aver.
SW UMa	–	–	–	–	–	–	−0.002	0.56	0.080	−7.18	–	–	0.017	−5.15	–	–	–	–			4	Sing. sp.
AN UMa	0.067	−2.81	–	–	–	–	–	–	0.008	−0.43	–	–	–	–	0.026	−3.56	–	–			2	Sp. 1
	0.026	−1.46	–	–	–	–	–	–	0.064	−5.20	–	–	–	–	–	–	–	–			2	Sp. 3
BC UMa	–	–	–	–	–	–	−0.002	2.53	–	–	–	–	–	–	–	–	–	–			3	Sp. 2
DV UMa	–	–	–	–	–	–	−0.004	3.60	0.023	−7.28	–	–	–	–	–	–	–	–			4	Sp. 1
	–	–	–	–	–	–	−0.002	2.91	–	–	–	–	–	–	–	–	–	–			4	Sp. 2
SS UMi	–	–	0.015	−3.46	–	–	–	–	0.032	−2.33	–	–	–	–	–	–	0.008	−2.68			1	Aver.
TW Vir	0.270	−1.28	0.021	−0.43	–	–	−0.022	0.56	0.534	−2.26	0.526	−2.06	–	–	–	–	0.117	−2.39			1	Sing. sp.
	–	–	−0.080	1.00	–	–	−0.022	0.32	–	–	–	–	0.022	−0.46	–	–	–	–			4	Aver.

Gaussians. Blended lines as a result of our low resolution are quoted only once. This applies to Ca II at λ3968 Å and Hϵ at λ3970 Å, and Ca II at λ8542 Å and Paschen 11 at λ8545 Å, where the total fluxes and equivalent widths are given in the Hϵ and Paschen 11 columns respectively.

Table A1 lists the objects in lexigraphical order. The equivalent widths are in Å, while the fluxes are given in units of 10^{-13} erg s^{-1} cm^{-2}.

This paper has been typeset from a TEX/LATEX file prepared by the author.